A Journal of the Gesellschaft Deutscher Chemiker

Angewandte International Edition GDCh Chemie

www.angewandte.org

Accepted Article

Title: An Isotope-Labeled Single-Cell Raman Spectroscopy Approach for Tracking the Physiological Evolution Trajectory of Bacteria toward Antibiotic Resistance

Authors: Kai Yang, Fei Xu, Longji Zhu, Hongzhe Li, Qian Sun, Aixin Yan, Bin Ren, Yong-Guan Zhu, and Li Cui

To be cited as: *Angew. Chem. Int. Ed.* **2023**, e202217412

Link to VoR: https://doi.org/10.1002/anie.202217412

WILEY-VCH

10.1002/anie.202217412

WILEY-VCH

RESEARCH ARTICLE

An Isotope-Labeled Single-Cell Raman Spectroscopy Approach for Tracking the Physiological Evolution Trajectory of Bacteria toward Antibiotic Resistance

Kai Yang,[a] Fei Xu,[a] Longji Zhu,[a] Hongzhe Li,[a] Qian Sun,[a] Aixin Yan,[b] Bin Ren,[c] Yong-Guan Zhu[a] and Li Cui*[a]

[a] Dr. K. Yang, F. Xu, Dr. L. Zhu, Dr. H. Li, Prof. Q. Sun, Prof. Y.-G. Zhu, and Prof. L. Cui
Key Lab of Urban Environment and Health, Fujian Key Laboratory of Watershed Ecology
Institute of Urban Environment, Chinese Academy of Sciences, Xiamen, 361021, China. E-mail: lcui@iue.ac.cn
[b] Prof. A. Yan
School of Biological Sciences
The University of Hong Kong
Pokfulam Road, Hong Kong, China
[c] Prof. B. Ren
State Key Laboratory of Physical Chemistry of Solid Surfaces, College of Chemistry and Chemical Engineering
Xiamen University
Xiamen, 361005, China

Supporting information for this article is given via a link at the end of the document.

Abstract: Understanding evolution of antibiotic resistance is vital for containing its global spread. Yet our ability to in situ track highly heterogenous and dynamic evolution is very limited. Here, we present a new single-cell approach integrating D_2O-labeled Raman spectroscopy, advanced multivariate analysis, and genotypic profiling to in situ track physiological evolution trajectory toward resistance. Physiological diversification of individual cells from isogenic population with cyclic ampicillin treatment is captured. Advanced multivariate analysis of spectral changes classifies all individual cells into four subsets of sensitive, intrinsic tolerant, evolved tolerant and resistant. Remarkably, their dynamic shifts with evolution are depicted and spectral markers of each state are identified. Genotypic analysis validates the phenotypic shift and provides insights into the underlying genetic basis. The new platform advances rapid phenotyping resistance evolution and guides evolution control.

Introduction

Rapid evolution of antibiotic resistance due to the widespread use of antibiotics is causing frequent antibiotic treatment failure and challenging modern medicine.[1] Antibiotic resistance has become one of the leading health threats around the world.[2] During antibiotic therapy, bacteria can evolve different strategies to survive lethal antibiotic treatment. Among these, resistance mutation is a common strategy that enables bacteria to grow in the presence of antibiotics. Yet bacteria can also switch to a tolerant phenotype to survive antibiotic attack without developing resistance. In contrast to resistance, antibiotic tolerant cells cannot replicate when antibiotics are present but resume growth when antibiotics are removed. They are thus the major cause of recurrent chronic infections in addition to resistance.[3] Moreover, the resulting antibiotic tolerant cells provide a viable pool facilitating the subsequent resistance evolution.[4] Therefore, understanding antibiotic tolerance and the trajectory toward resistance is crucial for developing efficient antibacterial therapies.

During the course of resistance evolution, antibiotic tolerance arises stochastically from a small subset of cells within an isogenic population due to phenotypic switching.[5] These growth-arrested tolerant cells are expected to undergo dramatic physiological responses to adapt to and survive the antibiotic exposure. Cyclic antibiotic administration has been demonstrated to increase the tolerant fraction of bacteria, indicating the dynamic phenotypic changes during treatment prior to the ultimate evolution of resistance.[6] Moreover, some recent works found alterations of expression in genes conferring antibiotic tolerance, such as toxin-antitoxin modules,[5-6, 7] stringent response,[8] quorum sensing modulates,[9] SOS response, [8b, 10] suggesting the complex responses of tolerant cells. Thus, tracking bacterial physiology in situ toward tolerance and resistance evolution will be valuable for developing diagnosis tools and reducing the rates of resistance evolution. Moreover, such phenotype interrogation will precede and complement the prevailing genotype interrogation.

Despite the importance of antibiotic tolerance, screening the small fraction of growth-arrested tolerant cells and tracking their physiological profiles from the large bacterial populations during resistance evolution are a grand challenge, largely due to the lack of tools that can sensitively monitor the phenotypic responses of individual cells in situ. By using time-lapse microscopy, Balaban *et al.* monitored the regrowth of tolerant cells after removal of antibiotic in microfluidic devices.[5] They further developed a colony analysis platform to detect and isolate the regrowing tolerant cells based on their longer lag time than sensitive cells.[6a, 11] However, these growth-based methods cannot directly monitor nongrowing tolerant cells in the presence of antibiotics. To understand the physiology of antibiotic tolerant cells in situ, several culture-independent single-cell techniques have been developed. For example, by constructing fluorescent reporter systems as proxies of tolerance-associated genes, the transcription/translation activity and their associated heterogeneity were monitored at the single cell level in situ.[12] However, these methods were inherently limited to measuring the expression of a few specific genes based on the predefined

10.1002/anie.202217412

WILEY-VCH

RESEARCH ARTICLE

phenotypic traits. Moreover, the introduction of reporter genes *via* genetic manipulation allows only model bacteria to be studied, thereby impeding its broad application on other phenotypes and bacteria. Therefore, an alternative single cell method capable of in situ and comprehensively monitoring the physiological responses is needed for tracking the resistance evolution trajectory.

Raman spectroscopy is an appealing single-cell technique for phenotypic analysis of microbial cells. Raman spectroscopy measures the vibrational energy of chemical bonds in a label-free manner and is informative of intrinsic biochemical profile of a microbial cell,[13] including proteins, nucleic acids, lipids, carbohydrates, pigments and metabolites. The rich chemical information provided by Raman spectroscopy enables resolving physiological responses of bacteria to various stresses on the basis of comprehensive molecular events rather than one particular indicator.[14] The development of multivariate statistical methods further advances the discrimination of even subtle spectral alterations resulting from physiological changes of bacteria.[14b-d] Its single-cell level detection also enables a high-resolution means to dissect heterogeneity between individual cells that are averaged by population measurements. Furthermore, when coupled with D_2O stable isotope labeling as a general metabolic activity probe, Raman spectroscopy can measure in situ activity of single bacterial cells in a quantitative manner regardless of their growth.[15] These merits indicate the great potential of single-cell Raman spectroscopy in identifying and tracking dynamic physiological changes of bacteria along the evolution to antibiotic tolerance and resistance.

Here, we present a new single-cell platform that integrates Raman phenotypic profiling, isotope labeling, advanced multivariate analysis, and genotypic profiling to track the physiological and genomic evolutionary trajectories toward antibiotic tolerance and resistance in situ. A multiple cyclic and intermittent exposure to therapeutic doses of antibiotics was performed to enable development of antibiotic resistance. Raman spectroscopy combined with D_2O detected an increased tolerance to antibiotics with the treatment cycles. A further analysis of the entire spectral region with the advanced uniform manifold approximation and projection (UMAP) classified all the individual cells along the evolution to four subpopulations on the basis of their in situ physiological responses. Notably, the dynamic shift of bacterial physiology from ancestral cells to the evolved tolerant and resistant subpopulations was clearly depicted for the first time. Genotypic analysis of bacterial whole genome validated the observed phenotypes and provided deep insights into the underlying genetic basis. Furthermore, spectral markers specific to the four subpopulations representing different physiology states were identified. This work achieves in situ tracking physiological trajectory toward resistance evolution. The new platform is of great help for rapid and precise diagnosis of tolerance, guiding efficient therapy and containing the rates of resistance evolution.

Results and Discussion

Cyclic Antibiotic Treatments Lead to Antibiotic Resistance

To simulate the antibiotic treatment protocol in clinical settings, a therapeutic dose of ampicillin (50 μg mL^{-1}), which is ~ 8-fold minimum inhibitory concentration (MIC), was intermittently applied to antibiotic sensitive *E. coli* for 5 h followed by an overnight culture in ampicillin-free media (Figure 1A). A total of 10 cycles at daily intervals were applied until antibiotic resistance defined by clinical standards was established, i.e., reduced inhibition zone from 23 to 10 mm via a disk diffusion assay (Figure 1B and C). To illustrate the path to antibiotic resistance, MIC against ampicillin in batch cultures after each cycle of antibiotic treatment was examined. The MIC of evolved batch cultures relative to that of ancestors exhibited almost no change after 1-8 cycles of antibiotic exposure (Figure 1D), ruling out the evolution of antibiotic resistance. Significant increase of MIC reaching at least 6 and 16-fold of ancestral MIC was observed after 9 and 10 cycles (P < 0.001) respectively (Figure 1D), indicating the development of antibiotic resistance. In addition, although ampicillin is a bactericidal antibiotic by inhibiting cell wall synthesis, we observed that the bacteria with intact cell morphology increased after 6-8 cycles of 50 μg mL^{-1} ampicillin treatment, suggesting the possible adaptative evolution of antibiotic tolerance (Figure S1).

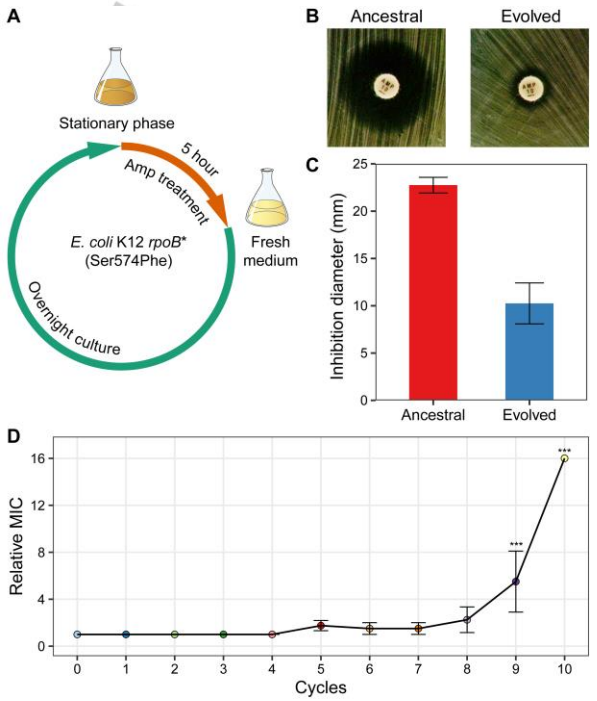

Figure 1. Cyclic antibiotic treatments lead to antibiotic resistance. (A) Schematic of the evolution experiment including 5 h of cyclic antibiotic exposure followed by an overnight culture to stationary phase. (B) Images and (C) diameters of disk diffusion inhibition zone of ancestral and evolved strain from three biological replicates. (D) Relative MIC fold increases in evolving batch culture. Significant differences between ancestral and each evolved cycle were marked as *** (P < 0.001, repeated measures ANOVA with Dunnett post-hoc correction).

Tracking Single-Cell Metabolic Activity Changes during Resistance Evolution

10.1002/anie.202217412

WILEY-VCH

RESEARCH ARTICLE

To detect the viable cells within the isogenic population and their tolerance to antibiotics, D_2O-labeled single-cell Raman spectroscopy (Raman-D_2O) was employed in a culture-independent manner to monitor the metabolic activity of cells in situ. C-D bands from the incorporation of D_2O-derived deuterium into *de novo* synthesized biomass can act as a quantitative probe of microbial activity.[15b, 16] Figure 2A shows the average spectra and their standard deviation (sd) from around 1250 individual cells after 0 to 10 cycles of antibiotic exposure. Both the C-D bands and fingerprint region displayed some changes. Figure 2B shows the corresponding CD ratios (CD/(CD+CH)) from these individual cells. A large variation of metabolic activities at each cycle and their dynamic increase with treatment cycles were observed. To interrogate these changes, all the single cells were categorized into three subsets with no, low and high metabolic activity based on their CD ratios. No metabolic activity (CD ratio < 4.04%, blue line) was determined as those below the mean + 3× sd of D-free cells; high metabolic activity (CD ratio > 12.11%, orange line) was defined as those above the mean + 3 × sd of ancestral cells (cycle 0), and low metabolic activity was those in between. Clearly, these cells at each cycle were not in the identical state but had a notable heterogeneity in metabolic activity, illustrating an important physiological change of bacteria to survive antibiotic treatment. Although there are always some cells with completely inhibited activities in each cycle, those with low or high activity tolerated and survived the lethal dose of ampicillin treatment.[17]

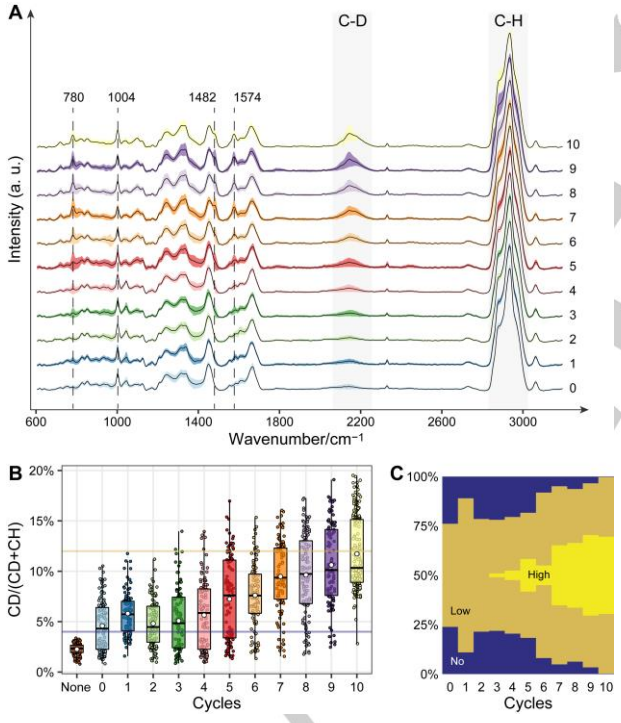

Figure 2. Dynamics of bacterial metabolic activity under ampicillin stress during evolution. (A) Single-cell Raman spectra of bacteria during evolution under 0-10 cycles of ampicillin treatment. Means and standard deviations (sd) were depicted as solid line and light shade, respectively. (B) Dynamic of single-cell metabolic activity under ampicillin treatment in ancestral and evolving batch culture as revealed by single-cell Raman with D_2O labeling. Each point is a measurement of a single cell, and box plots indicate quartiles of each evolved population. None is from D-free bacteria. (C) The proportion of no, low, and high metabolic activity cells in bacterial population during evolution. The threshold values of low (~ 4.04%) and high (~ 12.11%) metabolic activity were determined as mean+3 sd of CD ratios of unlabeled cells and ancestral cells, respectively.

The proportion of no, low, and high metabolic activity cells in bacterial population during evolution was calculated and shown in Figure 2C. Of note, ampicillin-sensitive ancestral bacteria at 0 cycle displayed both no and low activity, indicating the presence of phenotypically tolerant cells, consistent with previous findings that sensitive cells can partially maintain a certain level of metabolic activity to tolerate lethal antibiotics.[15a, 18] After 1-8 cycles of antibiotic exposure, although the MICs of evolved batch culture were still at the same low level as that of ancestral strains (P > 0.05, Figure 1D), the metabolic activity increased gradually. Specifically, the tolerant subpopulation with high metabolic activity (light yellow) emerged after 3 cycles of ampicillin exposure and kept increasing, while the proportion of sensitive cells with no metabolic activity (navy blue) gradually decreased with evolution (Figure 2C). The fact of increased metabolic activity preceding MIC upshift revealed that an enhanced antibiotic tolerance occurred in bacteria in order to adapt to antibiotic stress even without developing resistance. When an elevated MIC was detected after 9 and 10 cycles (Figure 1D), nearly all the bacteria were metabolically active under ampicillin treatment and the abundance of high metabolic activity subpopulation reached the highest. These results demonstrated the strong capability of single-cell Raman-D_2O to reveal the in situ metabolic activity of even growth-arrested tolerant cells. Considering that tolerance can dramatically affect antibiotic efficacies but is often overlooked in the clinic, Raman-D_2O also offers a rapid and precise tool to screen and predict antibiotic tolerance to guide antibiotic therapy.

Capturing Single-Cell Physiological Shift from Tolerance to Resistance

The increasing antibiotic tolerance with antibiotic treatment cycles indicated that bacteria may adjust their physiological states to adapt to antibiotic stress. To clarify this, Raman fingerprint regions that provide rich intrinsic biochemical information of cells were analyzed to examine bacterial physiological responses to antibiotics during resistance evolution with greater details. Here, the 1250 single-cell spectra with each containing 467 Raman bands (based on a spectral resolution of ~2.5 cm^{-1} in the range of 600 to 1800 cm^{-1}) from all the exposure cycles were analyzed. Due to the high dimension of Raman bands in the fingerprint region, unsupervised UMAP algorithm was performed for dimensionality reduction and spectra clustering according to their similarities (Figure 3A-L). UMAP is constructed from a theoretical framework based on Riemannian geometry and algebraic topology. While UMAP has been successfully applied for interpretation and visualization of single-cell gene expression data,[19] an early application was for the molecular spectra analysis.

A large-scale physiological atlas including all treatment cycles was generated. According to the clustering pattern of UMAP, all spectra were segregated into four branches (Figure 3B), indicating there were four subpopulations with distinctive phenotypic responses during the evolution. The corresponding single-cell CD ratios were also shown (Figure 3A). Interestingly, all cells defined with no activity were clustered to Branch A while the high-activity cells were to Branch D. The low-activity cells were distributed in both Branch B and C, indicating the different physiological responses exhibited by these two subpopulations.

10.1002/anie.202217412

WILEY-VCH

RESEARCH ARTICLE

To facilitate visualizing the differences and shifts of physiological responses with resistance evolution, each of the evolved cycle (1-10) was compared with 0 cycle from the ancestral strain, respectively. In the early 1 to 2 cycles (Figure 3C-D), most of the spectra were clustered primarily into Branch A and B, consistent with the metabolic activity and MIC results that intrinsically sensitive (Sensitive, Branch A) and intrinsically tolerant (Tolerant 1, Branch B) subpopulations coexisted. With the progress of evolution (3-7 cycle) especially after cycle 5, more spectra moved to Branch C, meanwhile the spectra in Branch A with no metabolic activity decreased (Figure 3E-I). Considering that MIC was still the same as the sensitive strain, this result indicated the evolution of a new tolerant subpopulation (Tolerant 2) in Branch C with a potentially different physiological responses from Branch B. After 8 cycles of exposure (Figure 3J-L), more and more spectra moved to Branch D with the high activity and those in Branch A and B dropped. After 10 cycles, almost all the bacterial cells were clustered into Branch C and Branch D (Figure 3L). Because MIC increased significantly after 9 cycles, this result indicated mixed tolerant and resistant (Resistant, Branch D) cells in cycle 10 and the evolution of resistant subpopulation on the basis of the evolved tolerant subpopulation.

So, here, we depicted a very detailed trajectory illustrating the diversification of physiology from one isogenic population to four subpopulations, and their dynamic shifts from intrinsic sensitivity and tolerance to evolved tolerance and resistance (Figure 3M).

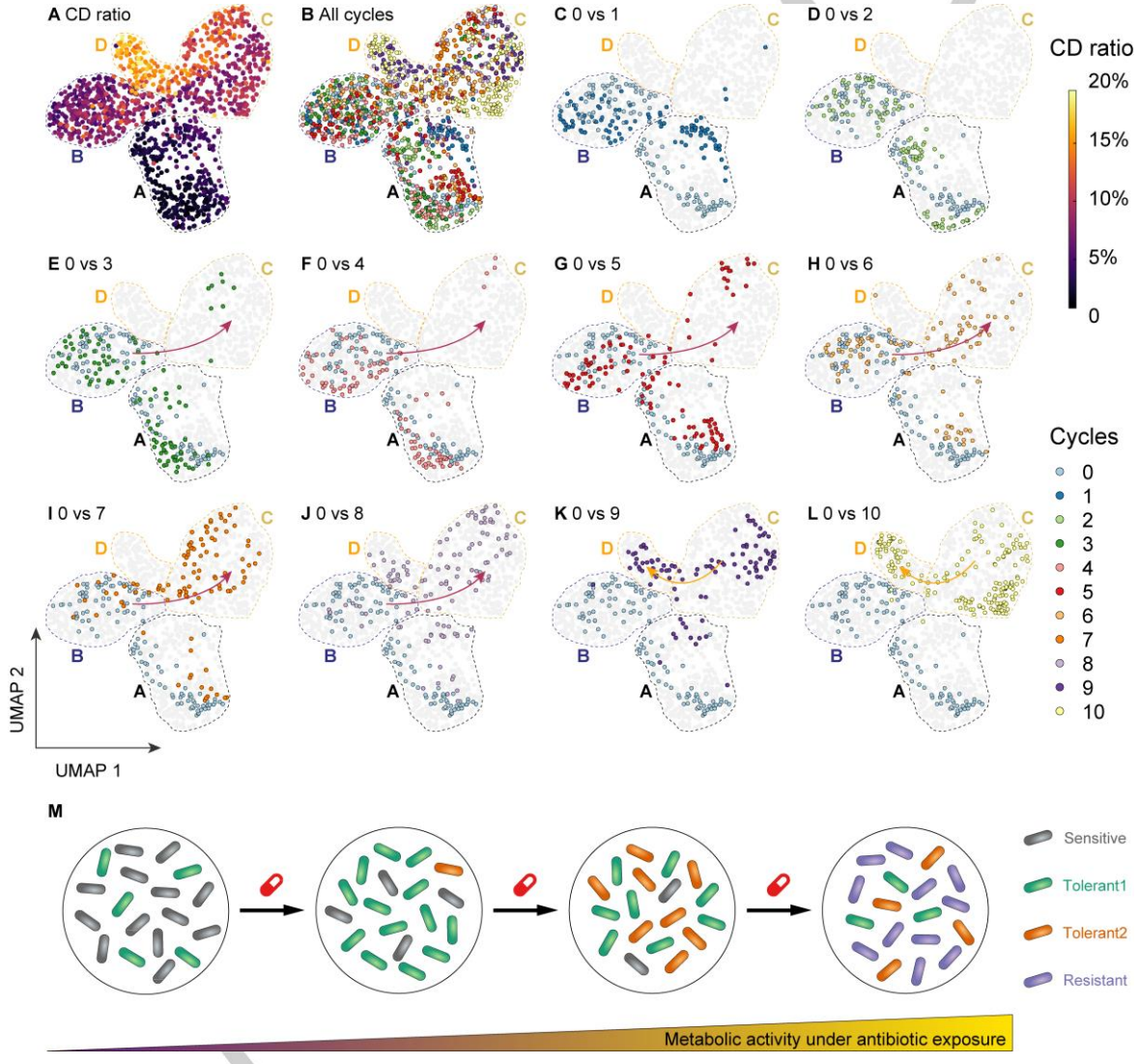

Figure 3. UMAP representation of phenotypic responses based on the whole Raman fingerprint region of all individual cells under ampicillin treatment. Each point is a measurement of a single cell. Bacterial cells are colored by metabolic activity (A), or cycles of treatment (B-L) in the evolved batch cultures. UMAP plots from C to L compare the ancestral cell with the evolved cells after each treatment cycle, respectively. (M) Conceptual model showing the physiological evolution trajectory from the ancestral Sensitive and Tolerant 1 cells to the evolved Tolerant 2 and Resistant cells.

Such physiological diversification of individual cells is important for maintaining the survival of the entire bacterial population when facing unpredictable stress such as antibiotics.[20] Although tolerance evolution prior to resistance development has been previously reported ex situ by sequencing bacterial isolates from different evolution stages,[4a, 21] this is the first time that

10.1002/anie.202217412

physiological trajectory toward resistance evolution was illustrated on the basis of the in situ phenotypic responses. Compared with fluorescence-based methods that determined only a limited category of phenotypic traits, such as translation activity of *rrnB* gene,[12a] the measurement of physiological responses that represent the overall cell state enables subtle cellular changes to be discerned in individual bacteria. Understanding such phenotypic diversification has important clinical implications for guiding effective antibacterial therapies to target antibiotic tolerant state to prevent the further evolution to resistance.

Moreover, leveraging the merit of single-cell resolution, intercellular phenotypic heterogeneity within one population was quantified by calculating the cell-to-cell Euclidean distance (Figure 4). The distribution histograms of intercellular Euclidean distances displayed a dynamic change with the cyclic antibiotic exposure. Compared with the ancestral strain (cycle 0), bacterial population seemed to decrease its heterogeneity in cycle 1. While from cycle 2 to 8, the heterogeneity increased as observed from the increased cell-to-cell distance. After continuing the evolution for 9 and 10 cycles, the heterogeneity of the bacterial population decreased. The reason was at least partially attributed to the variations among cells in gene expression, protein synthesis and ATP levels. Similar phenomena were observed previously in other phenotypes of bacteria during resistance evolution, such as single-cell lag time that sets the fitness of population.[4b, 6a] The variance in the lag time increased at the early stage but then decreased when a strain with the maximum fitness dominated the whole population.[4b] Such phenotypic heterogeneity increases the probability of entire population to develop different survival strategies against antibiotics and facilitates the adaptive evolution of resistance.[22]

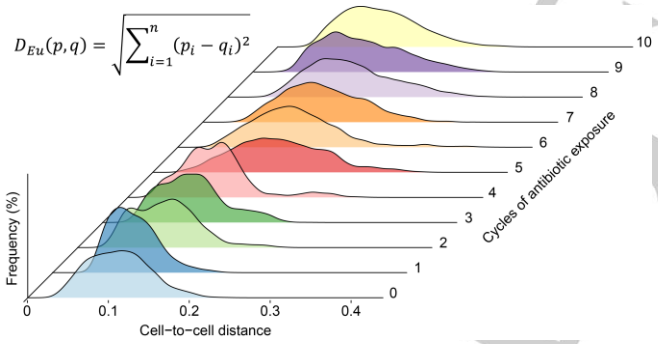

Figure 4. Distribution of cell-to-cell Euclidean distances during evolution. The frequency represents the normalized proportion of cell-to-cell distance in ancestral and evolved batch cultures.

Genotypic Basis Underlying Tolerance and Resistance Phenotype

To validate the finding of phenotypic shifts based on single-cell Raman interrogation and understand the associated genetic basis, whole genome sequencing (WGS) was conducted on all the ancestral and evolved bacteria subjected to 1-10 cycles of antibiotic exposure. As shown in Figure S2, all of the evolved bacteria harbored identical genes of *ydcI* (Δ11bp), *rpoB* (S574F), and *ompN* (T186I) to that of ancestral strain, indicating that they were inherited from the ancestor bacteria and ruling out bacterial contamination (Table S1). Among them, *ydcI* gene deletion (Δ11bp) was recently reported to increase the frequency of antibiotic tolerant cells,[23] explaining the coexistence of Sensitive (Branch A) and Tolerant 1 subpopulation (Branch B) in the ancestral strain revealed by both activity (Figure 2) and physiological responses (Figure 3). With the progress of cyclic treatment, new mutation of *ydfV* gene started to show up in the evolved populations of cycle 3, and its abundance kept increasing until cycle 8 (Figure 5A). The mutation of *ydfV* (IS2) was located in the promotor of *relBE* module (Figure 5B) that encoded type II toxin-antitoxin systems and was reported to confer antibiotic tolerance when overexpressed.[24] Of note, this tolerance mutation of *ydfV* emerged simultaneously with the newly evolved Tolerant 2 subpopulations in Branch C identify by Raman (Figure 3E-I). After 9 and 10 cycles when MIC increased significantly by 6 to 16 folds, resistance mutation in *galU* genes (IS4 in *galU* gene) emerged and coexisted with the tolerance gene of *ydfV* (Figure 5A and S2). This was also consistent with the Raman phenotypic finding that both the evolved Tolerant 2 and Resistant become dominant in the population (Figure 3K and 3L). The *galU* gene mutation endows ampicillin resistance by insertional sequence of IS4,[25] thereby affecting outer membrane barrier properties and antibiotic permeation by altering lipopolysaccharides composition.[26] This is different from previously reported ampicillin-resistant mutation that was mostly restricted to *ampC* promoter encoding hyperproduction of β-lactamase.[4a, 27] In addition to sequencing the whole population of each cycle, WGS of tolerant and resistant isolates was also performed to further verify the population genomic findings. Tolerant strains of small colony variants were isolated from cycle 7 (C7_S) based on their prolonged bacterial lag time according to previously reported method.[4a, 28] Resistant strains were isolated from cycle 10 (C10_1 and C10_2) using selective ampicillin plate. As expected, the tolerance-associated mutation in *ydfV* and resistance mutation in *galU* were detected in the ampicillin tolerant and resistant strains, respectively, but not in ancestral strain (Figure 5C).

Overall, the genotypic analysis well validated the phenotypic diversification and dynamic shift from the original sensitivity and intrinsic tolerance to the evolved tolerance and eventually resistance identified by single-cell Raman physiology analysis. The genomic determinants underlying the observed phenotypes were also deciphered. These genotypic and phenotypic results clearly indicated the evolutionary adaptation of bacteria to cope with antibiotic stress by developing tolerance and then resistance, consistent with previous findings that tolerance preceded resistance.[4a] When facing antibiotic challenges, such phenotypic plasticity enables subpopulations of a species to survive, thereby sparing time for genotypic resistance mutations to arise. Compared with genotypic analysis, the phenotypic responses illustrated by Raman at the single-cell level facilitated a more rapid and in situ diagnosis of tolerant subpopulations.

10.1002/anie.202217412

WILEY-VCH

RESEARCH ARTICLE

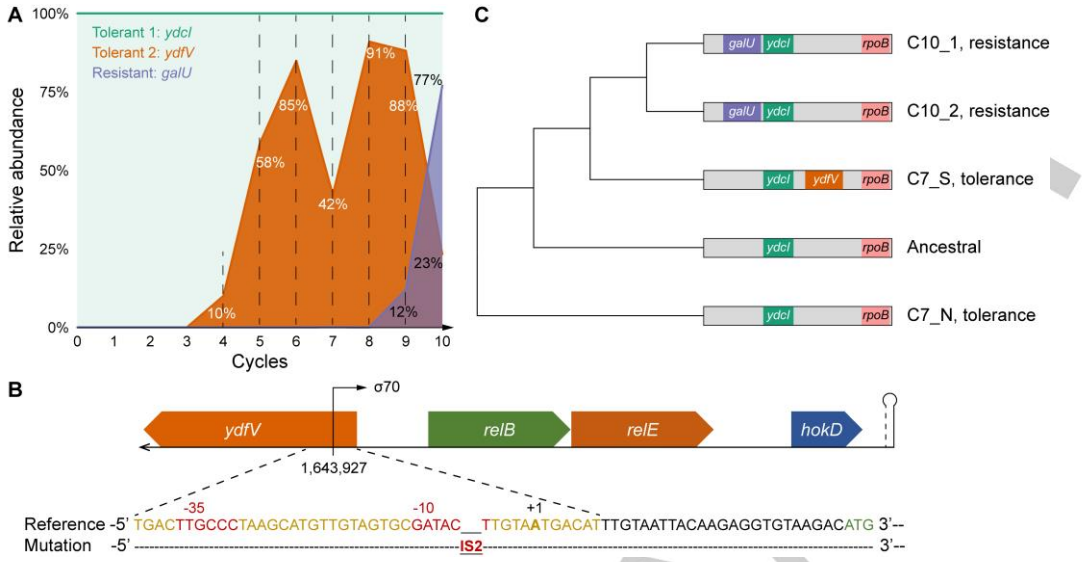

Figure 5. Genotypic basis underlying tolerance and resistance phenotype. (A) Relative abundance of background (*ydcI*), tolerance (*ydfV*) and resistance (*galU*) mutations in ancestral and evolved populations. (B) Tolerance mutation of *ydfV* was located in *relBE* module promotor region detected by whole genome sequencing. Red letters presented the position of promotor from -35 to -10 region. Antibiotic tolerance is conferred by insertional sequence (IS2) in the promoter. (C) Mutations identified by whole genome sequencing of bacterial isolates of ancestral, cycle 7 and cycle 10. Phylogenetic analysis suggests that they all originated from clonal evolution of the ancestral strain. C7_S, small colony variant isolated from cycle 7. C7_N, normal colony isolated from cycle 7.

Mining Spectral Markers Associated with Antibiotic Tolerance and Resistance

The clear segregation of cells into four subpopulations enabled us to mine the spectral markers specific to each physiological state in one bacterial population under antibiotic treatment. Of note, this is not achievable for bulk methods such as transcriptomic or proteomics that provide comprehensive but average information of the whole population. Figure 6A shows the mean and sd of spectra from each of the four subpopulations. Distinct spectral features were clearly observed, especially for the evolved Tolerant 2 and Resistant subsets.

The major Raman bands contributing to the phenotypic differentiation of four subpopulations were further deciphered using principal component analysis-linear discriminant analysis (PCA-LDA) (Figure 6B and Table S2). These major bands included nucleic acids (721, 780, 1482, and 1574 cm^{-1}), carbohydrates (1043 cm^{-1}), proteins (1250, and 1662 cm^{-1}), and lipids (1451 cm^{-1}), indicating the broad involvement of diverse biomolecules in bacterial physiological responses. The dynamic changes of these major bands during evolution were semi-quantified by integrating their intensity (Figure 6C and S3). The Raman bands at 721, 780, 1482, and 1574 cm^{-1} from nucleobases [14a, 29] were significantly higher in Tolerant 2 and Resistant than that of Sensitive and Tolerant 1. The higher contents of nucleic acids in the evolved Tolerant 2 and Resistant may indicate the stimulation of gene expression by the lethal dose of antibiotics. In contrast, the intensities at 1043 cm^{-1} from carbohydrates (deformation vibration of C-O-H)[30] and 1451 cm^{-1} from lipids (deformation vibrations of CH_2 and CH_3)[30b, 31] displayed an opposite trend ($P < 0.01$, Figure 6C). Ampicillin is documented as a bactericidal antibiotic that triggers higher rates of ROS production, leading to widespread cellular damage and disfunction, and eventually cellular death.[32] When facing lethal ampicillin stress, the central carbon metabolites and phospholipid in the metabolism of sensitive bacteria were reported to elevate, explaining the observed higher level of carbohydrate and lipid in ancestral cells.[32] Moreover, the propensity of bacteria to diminish carbohydrates and lipids availability has been reported to link to the tolerance against antimicrobial therapy as an important mediator of transition to non-replicating states.[33] In addition, the peaks at 1662 cm^{-1} (amide I) and 1250 (amide III) from proteins [30b, 31] were lower in Resistant than other subpopulations. The reasons maybe due to that sensitive and tolerant bacteria were associated with greater intracellular accumulation of protein aggregation. We also notice that the nucleic acids content of Tolerant 2 is significantly higher than that of Tolerant 1, whereas carbohydrates and lipids display an opposite trend (Figure 6). A plausible explanation is that Tolerant 2 harbors a mutation in the promotor of *relBE* module, which inhibits global translation and results in the cellular accumulation of ribonucleic acids [24b]. In addition, Tolerant 2 showed higher metabolic activity than Tolerant 1 (Figure 3A), suggesting their intensive energy consuming that may lead to a decrease in energy-related compounds. More importantly, these bands with major contributions to discriminate the four subpopulations can be used as the spectral biomarkers to precisely discern different stages during resistance evolution and guide antimicrobial therapy, especially the important Tolerant that contribute to chronic infections and served as reservoir for the subsequent resistance development. Of note, the CD stretching region is also worth future exploration via spectral unmixing method [34], because it may contain additional information of protein and lipid metabolism associated with resistance evolution.

10.1002/anie.202217412

WILEY-VCH

RESEARCH ARTICLE

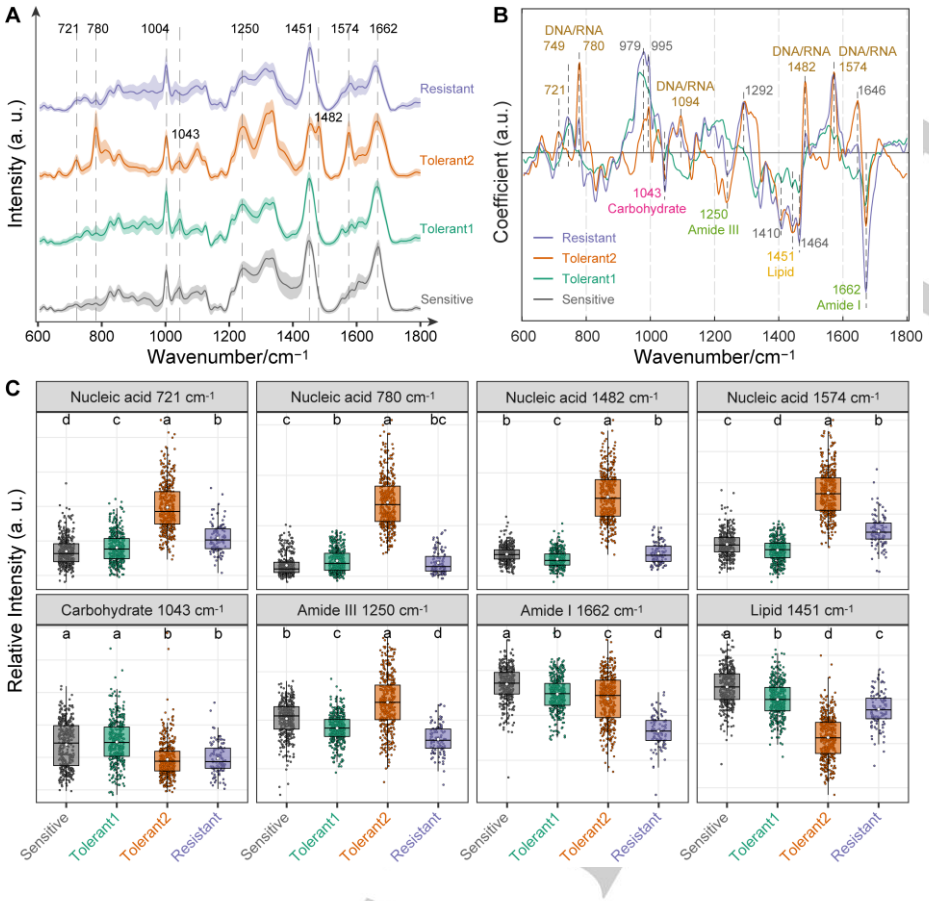

Figure 6. Identification of Raman spectral markers specific to each physiological state of bacteria during evolution. (A) Raman spectra of bacteria in four physiological states clustered by UMAP. Mean and sd was depicted as solid line and light shade, respectively. (B) PCA-LDA cluster vectors plot indicates the main Raman peaks contributing to the discrimination of physiology. (C) Relative intensity of major biomolecules in four physiological states. Each point is a measurement of a single cell, and box plots show the quartiles of each evolved population.

Conclusion

We developed a single-cell platform integrating Raman-D_2O phenotypic profiling, advanced multivariate analysis, and genotypic profiling for tracking physiological trajectory during the evolution toward antibiotic tolerance and resistance. In situ activity and physiology of individual cells, including those growth-arrested antibiotic tolerant cells in isogenic populations exposed to lethal antibiotics, were successfully detected in a culture-independent manner. The increased metabolic activity preceding MIC upshift revealed an enhanced antibiotic tolerance to antibiotic stress prior to resistance development. A further analysis of the entire spectra and their subtle changes with the advanced multivariate UMAP classified all the individual cells in one bacterial population into four subpopulations based on their in situ physiological responses. Remarkably, the dynamic shift from the intrinsic sensitive and tolerant subpopulations to the evolved tolerant and then resistant subpopulations with cyclic antibiotic treatment was clearly traced. Genotypic analysis of both bacterial populations and isolates via WGS validated the observed phenotypic changes and provided deep insights into the underlying gene mutations from tolerance to resistance. Furthermore, leveraging the clear segregation of subpopulations, spectral biomarkers specific to each physiological states in one bacterial population were mined, facilitating the precisely and rapidly discern of evolution stages. Heterogeneity of physiology was also quantified at the high-resolution single-cell level.

This is the first time that physiological trajectory toward antibiotic resistance evolution based on in situ phenotypic responses was revealed at the single-cell level. Such physiological diversification is critical for sustaining the survival of whole bacterial population when facing unpredictable stresses, but it was hard to be in situ captured previously by other methods and techniques. The method presented herein expands the arsenal and advances the deciphering of the heterogenous and dynamic phenotypic adaption over the course of antibiotic resistance evolution at the single-cell level. The rapid phenotypic adaption preceding resistance mutations revealed by single-cell Raman highlights its ability for early and precise antibiotic tolerance detections, thereby guiding antibacterial therapies to target tolerant state and containing the rate of further resistance evolution.

The integrated single-cell platform can be extended to a broad range of antibiotic and nonantibiotic chemicals and advance our understanding of how these chemicals promote resistance development. It is also possible to couple single-cell Raman with targeted single-cell sorting and multi-genomics to precisely link tolerant and resistant phenotype with genotype for an in-depth interrogation of evolution mechanisms.

Acknowledgements

This work was supported by Chinese Academy of Sciences (ZDBS-LY-DQC027), Natural Science Foundation of China (22176186, 21922608), Natural Science Foundation of Fujian Province (2022J05095), CAS Youth Interdisciplinary Team (JCTD-2021-13).

Keywords: Single cell Raman spectroscopy • antibiotic resistance • antibiotic tolerance • physiological response • evolution trajectory

[1] J. O'Neill, Review on Antimicrobial Resistance, **2014**.

[2] C. J. L. Murray, K. S. Ikuta, F. Sharara, L. Swetschinski, G. Robles Aguilar, A. Gray, C. Han, C. Bisignano, P. Rao, E. Wool, S. C. Johnson, A. J. Browne, M. G. Chipeta, F. Fell, S. Hackett, G. Haines-Woodhouse, B. H. Kashef Hamadani, E. A. P. Kumaran, B. McManigal, R. Agarwal, S. Akech, S. Albertson, J. Amuasi, J. Andrews, A. Aravkin, E. Ashley, F. Bailey, S. Baker, B. Basnyat, A. Bekker, R. Bender, A. Bethou, J. Bielicki, S. Boonkasidecha, J. Bukosia, C. Carvalheiro, C. Castañeda-Orjuela, V. Chansamouth, S. Chaurasia, S. Chiurchiù, F. Chowdhury, A. J. Cook, B. Cooper, T. R. Cressey, E. Criollo-Mora, M. Cunningham, S. Darboe, N. P. J. Day, M. De Luca, K. Dokova, A. Dramowski, S. J. Dunachie, T. Eckmanns, D. Eibach, A. Emami, N. Feasey, N. Fisher-Pearson, K. Forrest, D. Garrett, P. Gastmeier, A. Z. Giref, R. C. Greer, V. Gupta, S. Haller, A. Haselbeck, S. I. Hay, M. Holm, S. Hopkins, K. C. Iregbu, J. Jacobs, D. Jarovsky, F. Javanmardi, M. Khorana, N. Kissoon, E. Kobeissi, T. Kostyanev, F. Krapp, R. Krumkamp, A. Kumar, H. H. Kyu, C. Lim, D. Limmathurotsakul, M. J. Loftus, M. Lunn, J. Ma, N. Mturi, T. Munera-Huertas, P. Musicha, M. M. Mussi-Pinhata, T. Nakamura, R. Nanavati, S. Nangia, P. Newton, C. Ngoun, A. Novotney, D. Nwakanma, C. W. Obiero, A. Olivas-Martinez, P. Olliaro, E. Ooko, et al., *The Lancet* **2022**, *399*, 629-655.

[3] A. Brauner, O. Fridman, O. Gefen, N. Q. Balaban, *Nat. Rev. Microbiol.* **2016**, *14*, 320-330.

[4] a) I. Levin-Reisman, I. Ronin, O. Gefen, I. Braniss, N. Shoresh, N. Q. Balaban, *Science* **2017**, *355*, 826-830; b) J. Liu, O. Gefen, I. Ronin, M. Bar-Meir, N. Q. Balaban, *Science* **2020**, *367*, 200-204; c) E. M. Windels, J. E. Michiels, M. Fauvart, T. Wenseleers, B. Van den Bergh, J. Michiels, *ISME J.* **2019**.

[5] N. Q. Balaban, J. Merrin, R. Chait, L. Kowalik, S. Leibler, *Science* **2004**, *305*, 1622-1625.

[6] a) O. Fridman, A. Goldberg, I. Ronin, N. Shoresh, N. Q. Balaban, *Nature* **2014**, *513*, 418-421; b) B. Van den Bergh, J. E. Michiels, T. Wenseleers, E. M. Windels, P. V. Boer, D. Kestemont, L. De Meester, K. J. Verstrepen, N. Verstraeten, M. Fauvart, J. Michiels, *Nat. Microbiol.* **2016**, *1*, 16020.

[7] B. Van den Bergh, M. Fauvart, J. Michiels, *FEMS Microbiol. Rev.* **2017**, *41*, 219-251.

[8] a) D. Nguyen, A. Joshi-Datar, F. Lepine, E. Bauerle, O. Olakanmi, K. Beer, G. McKay, R. Siehnel, J. Schafhauser, Y. Wang, B. E. Britigan, P. K. Singh, *Science* **2011**, *334*, 982-986; b) A. Harms, E. Maisonneuve, K. Gerdes, *Science* **2016**, *354*.

[9] a) N. M. Vega, K. R. Allison, A. S. Khalil, J. J. Collins, *Nat. Chem. Biol.* **2012**, *8*, 431-433; b) N. Personnic, B. Striednig, E. Lezan, C. Manske, A. Welin, A. Schmidt, H. Hilbi, *Nat. Commun.* **2019**, *10*, 5216.

[10] F. Goormaghtigh, L. Van Melderen, *Sci. Adv.* **2019**, *5*, eaav9462.

[11] I. Levin-Reisman, O. Gefen, O. Fridman, I. Ronin, D. Shwa, H. Sheftel, N. Q. Balaban, *Nat. Methods* **2010**, *7*, 737.

[12] a) D. Shah, Z. Zhang, A. B. Khodursky, N. Kaldalu, K. Kurg, K. Lewis, *BMC Microbiol.* **2006**, *6*, 53; b) G. Manina, N. Dhar, J. D. McKinney, *Cell Host Microbe* **2015**, *17*, 32-46; c) K. Jun-Seob, Y. Ryota, S. Sooyeon, Z. Weiwei, W. T. K., *Environ. Microbiol.* **2018**, *0*.

[13] a) Y. Wang, W. E. Huang, L. Cui, M. Wagner, *Curr. Opin. Biotechnol.* **2016**, *41*, 34-42; b) L. Cui, H.-Z. Li, K. Yang, L.-J. Zhu, F. Xu, Y.-G. Zhu, *TrAC-Trend. Anal. Chem.* **2021**, *143*, 116415.

[14] a) L. Teng, X. Wang, X. J. Wang, H. L. Gou, L. H. Ren, T. T. Wang, Y. Wang, Y. T. Ji, W. E. Huang, J. Xu, *Sci. Rep.* **2016**, *6*, 34359; b) T. J. Moritz, D. S. Taylor, C. R. Polage, D. M. Krol, S. M. Lane, J. W. Chan, *Anal. Chem.* **2010**, *82*, 2703-2710; c) A. I. M. Athamneh, R. A. Alajlouni, R. S. Wallace, M. N. Seleem, R. S. Senger, *Antimicrob. Agents Ch.* **2014**, *58*, 1302-1314; d) T. J. Moritz, C. R. Polage, D. S. Taylor, D. M. Krol, S. M. Lane, J. W. Chan, *J. Clin. Microbiol.* **2010**, *48*, 4287-4290.

[15] a) H. Ueno, Y. Kato, K. V. Tabata, H. Noji, *Anal. Chem.* **2019**, *91*, 15171-15178; b) K. Yang, H.-Z. Li, X. Zhu, J.-Q. Su, B. Ren, Y.-G. Zhu, L. Cui, *Anal. Chem.* **2019**, *91*, 6296-6303; c) K. Yang, Q.-L. Chen, M.-L. Chen, H.-Z. Li, H. Liao, Q. Pu, Y.-G. Zhu, L. Cui, *Environ. Sci. Technol.* **2020**, *54*, 11322-11332.

[16] D. Berry, E. Mader, T. K. Lee, D. Woebken, Y. Wang, D. Zhu, M. Palatinszky, A. Schintlmeister, M. C. Schmid, B. T. Hanson, N. Shterzer, I. Mizrahi, I. Rauch, T. Decker, T. Bocklitz, J. Popp, C. M. Gibson, P. W. Fowler, W. E. Huang, M. Wagner, *Proc. Natl. Acad. Sci. U. S. A.* **2015**, *112*, E194-E203.

[17] S. Ronneau, P. W. S. Hill, S. Helaine, *Curr. Opin. Microbiol.* **2021**, *64*, 76-81.

[18] K. Lewis, *Annu. Rev. Microbiol.* **2010**, *64*, 357-372.

[19] E. Becht, L. McInnes, J. Healy, C.-A. Dutertre, I. W. H. Kwok, L. G. Ng, F. Ginhoux, E. W. Newell, *Nat. Biotechnol.* **2019**, *37*, 38-44.

[20] a) D. J. Kiviet, P. Nghe, N. Walker, S. Boulineau, V. Sunderlikova, S. J. Tans, *Nature* **2014**, *514*, 376; b) M. E. Lidstrom, M. C. Konopka, *Nat. Chem. Biol.* **2010**, *6*, 705-712.

[21] I. Santi, P. Manfredi, E. Maffei, A. Egli, U. Jenal, *Mbio* **2021**, *12*, e03482-03420.

[22] S. Moreno-Gámez, D. J. Kiviet, C. Vulin, S. Schlegel, K. Schlegel, G. S. van Doorn, M. Ackermann, *Proc. Natl. Acad. Sci. U. S. A.* **2020**, 202003331.

[23] S. M. Hingley-Wilson, N. Ma, Y. Hu, R. Casey, A. Bramming, R. J. Curry, H. L. Tang, H. Wu, R. E. Butler, W. R. Jacobs, A. Rocco, J. McFadden, *Proc. Natl. Acad. Sci. U. S. A.* **2020**, *117*, 4152-4157.

[24] a) M. Gotfredsen, K. Gerdes, *Mol. Microbiol.* **1998**, *29*, 1065-1076; b) I. Keren, D. Shah, A. Spoering, N. Kaldalu, K. Lewis, *J. Bacteriol.* **2004**, *186*, 8172-8180; c) E. Maisonneuve, L. J. Shakespeare, M. G. Jørgensen, K. Gerdes, *Proc. Natl. Acad. Sci. U. S. A.* **2011**, *108*, 13206-13211.

[25] a) K. G. Eriksson-Grennberg, K. Nordström, P. Englund, *J. Bacteriol.* **1971**, *108*, 1210-1223; b) H. S. Girgis, K. Harris, S. Tavazoie, *Proc. Natl. Acad. Sci. U. S. A.* **2012**, *109*, 12740-12745.

[26] a) J. Kurushima, H. Tomita, C. M. Dozois, *Appl. Environ. Microb.* **2021**, *87*, e02875-02820; b) C. Ching, M. H. Zaman, A. C. Gales, *mSphere* **2021**, *6*, e00778-00721.

[27] B. Jaurin, S. Normark, *Cell* **1983**, *32*, 809-816.

[28] C. Vulin, N. Leimer, M. Huemer, M. Ackermann, A. S. Zinkernagel, *Nat. Commun.* **2018**, *9*, 4074.

[29] J. De Gelder, K. De Gussem, P. Vandenabeele, L. Moens, *J. Raman Spectrosc.* **2007**, *38*, 1133-1147.

[30] a) C. Farber, D. Kurouski, *Anal. Chem.* **2018**, *90*, 3009-3012; b) K. C. Schuster, E. Urlaub, J. R. Gapes, *J. Microbiol. Methods* **2000**, *42*, 29-38.

[31] G. J. Puppels, F. F. M. de Mul, C. Otto, J. Greve, M. Robert-Nicoud, D. J. Arndt-Jovin, T. M. Jovin, *Nature* **1990**, *347*, 301-303.

10.1002/anie.202217412

[32] P. Belenky, J. D. Ye, C. B. M. Porter, N. R. Cohen, M. A. Lobritz, T. Ferrante, S. Jain, B. J. Korry, E. G. Schwarz, G. C. Walker, J. J. Collins, *Cell Rep.* **2015**, *13*, 968-980.

[33] J. M. Stokes, A. J. Lopatkin, M. A. Lobritz, J. J. Collins, *Cell Metabolism* **2019**, *30*, 251-259.

[34] L. Shi, C. Zheng, Y. Shen, Z. Chen, E. S. Silveira, L. Zhang, M. Wei, C. Liu, C. de Sena-Tomas, K. Targoff, W. Min, *Nat. Commun.* **2018**, *9*, 2995.

10.1002/anie.202217412

WILEY-VCH

RESEARCH ARTICLE

Entry for the Table of Contents

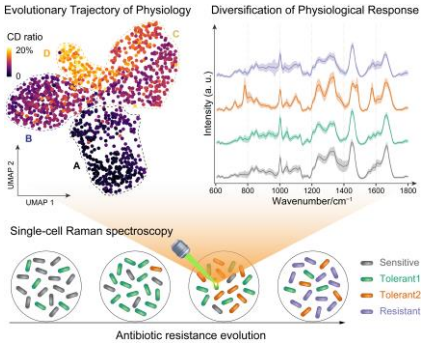

A single-cell approach integrating D_2O-labeled Raman spectroscopy, advanced multivariate analysis and genotypic profiling was developed to in situ track the highly heterogenous and dynamic physiological evolution trajectory of bacteria toward antibiotic resistance. The physiological diversification of single cells into four subpopulations preceding resistance from an isogeneic population was sensitively captured and their dynamic shift was tracked.

Institute and/or researcher Twitter usernames: Kai Yang @superahura